DOI:10.28974/idojaras.2026.2.4

IDŐJÁRÁS

Quarterly Journal of the HungaroMet Hungarian Meteorological Service
Vol. 130, No. 2, April – June, 2026, pp.151–167

An investigation of the angular distribution of the degree of polarization in natural solar radiation diffusely reflected and transmitted through atmospheric layers

Jurabek Y. Rozikov*, **Makhmud M. Sobirov**, **Valijon U. Ruziboyev**, and **Muhabbat M.Kamolova**

Department of Physics, Fergana State University
Fergana, 150100, Uzbekistan

**Correponding author E-mail: roziqovjurabek1991@gmail.com*

(Manuscript received in final form on June 23, 2025)

Abstract— This study investigates the angular distribution of the degree of polarization of diffusely reflected and transmitted natural solar radiation in atmospheric layers subjected to multiple Rayleigh scattering. The analysis employs the Chandrasekhar's S,T- matrix theory and the factorization method. Specific characteristics related to the numerical computation of *X* and *Y* functions using the successive approximations method are detailed. The results reveal that when the observation angle equals the illumination angle ($\mu = \mu_0$), a notable feature emerges in the angular distribution of the degree of polarization of diffusely transmitted light. At this juncture, a sharp change in the degree of polarization is observed. Additionally, the study examines the dependence of the angular width of this discontinuity on the illumination angle and optical thickness.

Key-words: polarization, optical thickness, S,T-matrices, X,Y-functions, neutral points

1. Introduction

Chandrasekhar's theory of $X(\mu), Y(\mu)$ functions (*Chandrasekhar*, 1960) is widely recognized as a key approach to investigate the transmission of polarized radiation in turbid, light-scattering media with limited optical thicknesses. It is extensively utilized in addressing diverse practical issues in the field of atmospheric physics. Extensive research has been conducted on the analytical properties of the $X(\mu)$ and $Y(\mu)$ functions, as well as on the numerical methods used to solve them. Nevertheless, the subject of $X(\mu), Y(\mu)$ functions remains pertinent and continues to captivate the interest of experts. The research of *Natraj et al.* (2009) and *Natraj* and *Hovenier* (2012) have demonstrated that the often utilized tables by Chandrasekhar and Coulson (*Chandrasekhar* and *Elbert,* 1954; *Coulson,* 1988; *Coulson et al.,* 1960), which are applied for solving practical problems in atmospheric physics, exhibit low accuracy and do not sufficiently characterize polarization phenomena. The authors performed novel numerical computations with enhanced precision. However, research focused on the examination of polarization phenomena in atmospheric layers and the use of polarization methods for remote sensing of the Earth's surface still relies on the works of Chandrasekhar and Coulson. These works serve as reference points for evaluating the outcomes of both theoretical and practical investigations (*Yan et. al.,* 2019; *Yan et. al.,* 2020; *Mishchenko,* 1987; *Mishchenko et. al.,* 2006).

A technique for solving the radiative transfer equation for polarized light in media with limited optical thickness using the factorization method was proposed in *Sobirov and Rozikov* (2020). This method aims to refine the theoretical framework and improve the precision of numerical calculations. The findings demonstrate that the factorization method significantly simplifies both the analytical and numerical computations involved in solving the radiative transfer equation for polarized radiation. Initially developed by *Lenoble* (1970), this approach was further elaborated upon in *Ivchenko et. al.* (1980), *Ivchenko et. al.* (1981), *Sobirov* and *Yuldashev* (1984), and *Pikus et. al.* (1985), and it was effectively applied to axisymmetric problems in crystals, particularly within the semi-infinite medium model. The present study investigates the angular distribution of the degree of polarization of diffusely reflected and transmitted natural solar radiation through atmospheric layers, considering multiple Rayleigh scattering. The analysis is grounded in the theoretical framework outlined in *Sobirov and Rozikov* (2020).

2. Equation for the reflection and transmission matrix

The radiative transfer equation (*Chandrasekhar*, 1960) describes the radiation field in a plane-parallel medium that scatters and absorbs light, without any internal sources, when it is lit by plane, monochromatic polarized radiation. The

equation can be written as follows:

$$\mu \frac{d\mathbf{I}(\tau,\mathbf{\Omega})}{\mathrm{d}\tau} = \mathbf{I}(\tau,\mathbf{\Omega}) - \frac{\widetilde{\omega}_0}{4\pi}\int_0^1 d\mu' \int_0^{2\pi} d\varphi' \, \mathbf{P}(\mathbf{\Omega},\mathbf{\Omega}')\mathbf{I}(\tau,\mathbf{\Omega}') - \\ - \frac{\widetilde{\omega}_0}{4}\exp\left(-\frac{\tau}{\mu_0}\right)\mathbf{P}(\mathbf{\Omega},\mathbf{\Omega_0})\mathbf{F}, \qquad (1)$$

where τ represents the optical thickness of the medium, $\widetilde{\omega}_0$ is the single scattering albedo (quantum yield of single scattering) calculated as $\frac{a^{\mathrm{sc}}}{\alpha^{\mathrm{ext}}+a^{\mathrm{sc}}}$, α is the attenuation coefficient (per unit volume) given by $\alpha = \alpha^{\mathrm{abs}} + a^{\mathrm{sc}}$, α^{abs} denotes the true absorption coefficient, a^{sc} represents the scattering coefficient, z is the axis directed normally from the surface of the medium, $\pi\boldsymbol{F}$ is the total flux of the incident parallel radiation per unit area (at the boundary $\tau = 0$), and $\boldsymbol{P}(\mathbf{\Omega},\mathbf{\Omega_0})$ is the Rayleigh phase matrix.

The intensity of radiation propagating in a medium, in the direction $\Omega = \Omega(\theta,\varphi)$ (where θ is the polar angle determined by the direction of the vectors $\boldsymbol{n^0}$ and Ω, $\boldsymbol{n^0}$ is the normal to the surface of the medium, and φ is the azimuthal angle), is described by the Stokes matrix (in the Chandrasekhar basis (*Chandrasekhar*, 1960)):

$$\mathbf{I} = \begin{bmatrix} I_l \\ I_r \\ U \\ V \end{bmatrix}, I_l = d_{ll}, I_r = d_{ll}, \mathrm{U} = 2\mathrm{Re}d_{lr}, V = 2\mathrm{Im}d_{lr}, \qquad (2)$$

where I_l and I_r are the intensities in the l and r polarizations, the unit orthogonal vector $\mathbf{l}$ lies in the plane of the vectors $\boldsymbol{n^0}$ and $\boldsymbol{\Omega}$, and $\boldsymbol{r}$ is perpendicular to it, $d_{ij} \approx \left(E_i, E_j^*\right)$. Here, $i,j = l,r,E_l$, and E_r are the corresponding components of the electric field of the light wave.

When the atmosphere is illuminated by natural, unpolarized solar radiation with a broad spectrum in the optical range, the optical thickness of the atmosphere varies depending on the wavelength of the light. In the radiative transfer equation (Eq.(1)), the optical thickness of the atmosphere τ is determined by the integral:

$$\tau(\lambda,z) = \int_0^\infty \alpha(\lambda,z)dz, \qquad (3)$$

where the integration is performed from sea level ($z = 0$) to the upper layers of the atmosphere, taking into account the change in air concentration with height. In the calculations presented below, the values of the optical thickness of the atmosphere are taken from *Coulson* (1988) according to the tables of Elterman (*Elterman,* 1968*; Pikus et. al.,* 1985). We present the values of optical thickness

for several wavelengths: $\tau = 0.01$ ($\lambda = 0.920$ μm), $\tau = 0.1$ ($\lambda = 0.546$ μm), $\tau = 0.15$ ($\lambda = 0.495$ μm), $\tau = 0.5$ ($\lambda = 0.371$ μm), and $\tau = 1$ ($\lambda = 0.312$ μm) at $\widetilde{\omega}_0 = 1$.

In the theory of S,T-matrices, the relationship between the intensities of diffusely reflected and transmitted radiation with the incident radiation is determined by the reflection and scattering matrices:

$$I_{\text{ref}}(\tau = 0, \Omega) = \left(\frac{\widetilde{\omega}_0}{4\mu}\right) S(\tau_1, \Omega, \Omega_0) F\left(\tau = 0, \overline{\Omega}_0\right). \quad (4)$$

$$I_{\text{trans}}\left(\tau = \tau_1, \overline{\Omega}\right) = \left(\frac{\widetilde{\omega}_0}{4\mu}\right) T(\tau_1, \Omega, \Omega_0) F\left(\tau = 0, \overline{\Omega}_0\right). \quad (5)$$

Using the principle of Ambartsumian's invariance and taking into account the boundary conditions from the radiative transfer equation (Eq.(1)), the general integral equations for the $\boldsymbol{S}$ and $\boldsymbol{T}$ matrices can be derived (*Chandrasekhar*, 1960):

$$\begin{aligned}\boldsymbol{S}(\tau_1, \Omega, \Omega_0) = \boldsymbol{Q}\left\{\left(\frac{3}{4}\right)\boldsymbol{S}^{(0)}(\tau_1, \mu, \mu_0) + \right.\\ +\sqrt{(1-\mu^2)(1-\mu_0^2)}\boldsymbol{S}^{(1)}(\tau_1, \Omega, \Omega_0)\boldsymbol{P}^{(1)}(\mu, \phi, -\mu_0, \phi_0) +\\ \left. S^{(2)}(\tau_1, \mu, \mu_0)\boldsymbol{P}^{(2)}(\mu, \phi, -\mu_0, \phi_0)\right\}. \quad (6)\end{aligned}$$

$$\begin{aligned}\boldsymbol{T}(\tau_1, \Omega, \Omega_0) = \boldsymbol{Q}\left\{\left(\frac{3}{4}\right)\boldsymbol{T}^{(0)}(\tau_1, \mu, \mu_0) + \right.\\ +\sqrt{(1-\mu^2)(1-\mu_0^2)}\boldsymbol{T}^{(1)}(\tau_1, \Omega, \Omega_0)\boldsymbol{P}^{(1)}(\mu, \phi, -\mu_0, \phi_0) +\\ \left. +T^{(2)}(\tau_1, \mu, \mu_0)\boldsymbol{P}^{(2)}(\mu, \phi, -\mu_0, \phi_0)\right\}. \quad (7)\end{aligned}$$

In Eqs.(1)–(7), the problem is presented in general form. In Eq.(1), all four components of the Stokes matrix are simultaneously determined, taking into account both linearly polarized and circularly polarized radiation. For brevity, we will discuss the solution of the problem concerning only the I_l and I_r components of the Stokes matrix, as we are considering the case where the medium is illuminated by unpolarized radiation.

To solve this problem, it is sufficient to consider the 2x2 block matrices in the $\boldsymbol{S}$ and $\boldsymbol{T}$ matrices in Eqs. (6) and (7). For brevity, we will not go into detail describing each term in Eqs. (6) and (7) (see *Sobirov* and *Rozikov*, 2020).

In the factorization method, the values of the $\boldsymbol{S}^{(0)}$ and $\boldsymbol{T}^{(0)}$ matrices in Eqs. (6) and (7) are determined by solving the system of equations for the $\boldsymbol{X}^{(0)}$ and $\boldsymbol{Y}^{(0)}$ matrices, which are 2x2 matrices with eight components:

$$\boldsymbol{X}^{(0)}(\mu) = \mathbf{1} + \mu\widetilde{\omega}_0 \int_0^1 \frac{d\mu'\Psi(\mu')}{\mu+\mu'}\left[\boldsymbol{X}^{(0)}(\mu)\boldsymbol{X}^{(0)^+}(\mu') - \boldsymbol{Y}^{(0)}(\mu)\boldsymbol{Y}^{(0)^+}(\mu')\right]. \quad (8)$$

$$\boldsymbol{Y}^{(0)}(\mu) = \mathbf{1}\exp\left(-\frac{\tau_1}{\mu}\right) + \mu\widetilde{\omega}_0 \int_0^1 \frac{d\mu'\Psi(\mu')}{\mu-\mu'}\left[\boldsymbol{Y}^{(0)}(\mu)\boldsymbol{X}^{(0)^+}(\mu') - \right.$$
$$\left. - \boldsymbol{X}^{(0)}(\mu)\boldsymbol{Y}^{(0)^+}(\mu')\right]. \quad (9)$$

Here, the identity matrix has a dimension of 2x2. The $\boldsymbol{S}^{(1)}$, $\boldsymbol{T}^{(1)}$, $\boldsymbol{S}^{(2)}$, and $\boldsymbol{T}^{(2)}$ matrices are determined through scalar functions $S^{(1)}$, $T^{(1)}$, $S^{(2)}$, and $T^{(2)}$, which, in turn, are determined by scalar integral equations for the $X(\mu)$ and $Y(\mu)$ functions, similarly to Eqs. (8) and (9), but using different characteristic functions.

According to Chandrasekhar's calculation method, the values of the $\boldsymbol{S}^{(0)}$ and $\boldsymbol{T}^{(0)}$ matrices are determined using four $X(\mu)$ and $Y(\mu)$ functions. However, this requires additional and complex calculations.

2.1. Iterative convergence of X and Y functions in a conservative medium when $\widetilde{\omega}_0 = 1$

Below are the results of numerical calculations of the $X(\mu)$ and $Y(\mu)$ functions obtained using the method of successive approximations or iterations. In the iteration method for solving Eqs. (3) and (4), the solution can be represented as a series in powers of $\widetilde{\omega}_0$ (*Lenoble,* 1970 and *Pikus et. al.,* 1985):

$$\boldsymbol{I}_{\text{ref}}(\tau_1 = 0, \Omega) = \sum\left(\frac{\widetilde{\omega}_0^n}{4\mu}\boldsymbol{S}^{(n)}(\tau_1, \overline{\Omega}, \Omega_0)\boldsymbol{F}\right), \quad (10)$$

$$\boldsymbol{I}_{\text{trans}}(\tau_1, \Omega) = \sum\left(\frac{\widetilde{\omega}_0^n}{4\mu}\boldsymbol{T}^{(n)}(\tau_1, \Omega, \Omega_0)\boldsymbol{F}\right), \quad (11)$$

where n is the order or multiplicity of scattering (*Mishchenko et.al.,* 2006; *Sobirov* and *Rozikov*, 2020; *Lenoble*, 1970; *Ivchenko et.al.,* 1980, 1981). The $\boldsymbol{S}^{(n)}(\tau_1, \Omega, \Omega_0)$ and $\boldsymbol{T}^{(n)}(\tau_1, \Omega, \Omega_0)$ are determined by solving the $\boldsymbol{S}$ and $\boldsymbol{T}$ matrices, expressed through integral equations for the $X(\mu)$ and $Y(\mu)$ functions using the method of successive approximations. If trial functions such as $\boldsymbol{X}(\mu) = 1$ and $\boldsymbol{Y}(\mu) = \mathbf{1}\exp(-\tau_1/\mu)$ are used, then after the first iteration, the intensity and polarization of singly scattered radiation are determined. After the first iteration, the scattering order does not correspond to the number of iterations. In the second approximation, the values of $X(\mu)$ and $Y(\mu)$ include contributions from singly, doubly, and partially triply scattered radiation, and so on.

Analytically, in Eq.(10), components up to the fourth order of scattering can

be distinguished, after which it becomes more complex. However, this is sufficient for the initial analysis of the physical picture of the formation of the intensity and polarization of secondary radiation. It is possible to establish a relationship between the number of iterations and the maximum order of scattering corresponding to this number of iterations. If $\tilde{n}$ is the number of iterations and n is the maximum order of scattering, then $\tilde{n} = 1, n = 1; \tilde{n} = 2, n = 3; \tilde{n} = 3, n = 7; \tilde{n} = 4, n = 15; \tilde{n} = 5, n = 31; \tilde{n} = 6, n = 63$, etc.

The solutions to the system of nonlinear integral equations for the $X(\mu)$ and $Y(\mu)$ functions were conducted at 201 points of μ values in the interval [0,1] through numerical calculations. Additionally, to compare our results with Chandrasekhar's tables, calculations were performed at fifty-one points.

To ensure the correctness of the numerical calculations, two conditions must be met (*Chandrasekhar*, 1960):

$$X(\mu) \to H(\mu), Y(\mu) \to 0 \text{ as } \tau \to \infty. \tag{12}$$

$$X(\mu) \to 1, Y(\mu) \to 1\exp(-\tau_1/\mu) \text{ as } \tau \to 0. \tag{13}$$

Indeterminacies of the type $0/0$ arising in Eq.(9) when $\mu - \mu' = 0$ are eliminated using Lopital's rule.

Numerical calculations showed that in the region $\widetilde{\omega}_0 < 0.7$, after a certain number of iterations, the values of all X and Y functions reach saturation and have good convergence at $\tau_1 \leq 1$ (*Sobirov et al.,* 2021; *Sobirov et al.,* 2023; *Sobirov et al.,* 2024). In the region $0.7 < \widetilde{\omega}_0 \leq 1$, convergence slows down, but depending on the optical thickness, the values of the *X* and *Y* functions approach the tabulated values of Chandrasekhar in *Chandrasekhar* and *Elbert* (1954). For example, at $\tau_1 = 0.15$ after the fifth iteration, and at $\tau_1 = 1$, after the fourth iteration. At small values of optical thickness, when $\tau_1 < 0.5$, the difference in some points is a maximum of 1%, and at $\tau_1 = 1$, it points up to 4%.

If in the case of $\tau_1 = 1$ the number of iterations is increased to $\tilde{n} = 5$, then near the point $\mu = 1$, in a narrow region $\Delta\mu$, the component $Y_{21}(\mu)$ takes negative values, which contradicts the conditions specified in Eq.(13). This means that at values of μ within $\Delta\mu$, the component $Y_{21}(\mu)$ has no solution. Considering that all $X_{11}, X_{12}, X_{21}, X_{22}, Y_{11}, Y_{12}, Y_{21}, Y_{22}$ functions form a single system of equations, all members of this system within $\Delta\mu$ also have no solution. It can be said that with the number of iterations $\tilde{n} = 4$, the values of all $X_{11}, X_{12}, X_{21}, X_{22}, Y_{11}, Y_{12}, Y_{21}, Y_{22}$ functions within $\Delta\mu$ reach saturation. In the subsequent iteration step (at $\tilde{n} = 5$), the values of these functions remain unchanged. However, in the region $1 - \Delta\mu$, the values of the $X_{11}, X_{12}, X_{21}, X_{22}, Y_{11}, Y_{12}, Y_{21}, Y_{22}$ functions increase. Increasing the number of iterations leads to the expansion of the $\Delta\mu$ region, and after two or three more iterations, $\Delta\mu$ covers the entire region $0 \leq \mu \leq 1$. The values of the $X(\mu)$ and

$Y(\mu)$ functions are determined by the iteration method according to the described scheme. A change in the sign of the $Y_{21}(\mu)$ component to negative indicates the achievement of the maximum number of iterations that determine the numerical values of the $X(\mu)$ and $Y(\mu)$ functions. The $X^{(1)}(\mu), Y^{(1)}(\mu), X^{(2)}(\mu), Y^{(2)}(\mu)$ functions show good convergence during iterations, regardless of the τ_1 value. After a certain number of iterations, they reach saturation and with an error of up to 1% coincide with the tabulated values in *Chandrasekhar* and *Elbert* (1954).

For comparison, Chandrasekhar's $\psi, \phi, \chi, \xi, \varepsilon, \eta, \sigma, \theta$ functions were converted into $X_{11}, X_{12}, X_{21}, X_{22}, Y_{11}, Y_{12}, Y_{21}, Y_{22}$ functions, and the following relationships exist between them:

$$X_{11} = \chi, X_{12} = \sqrt{2}\xi, X_{21} = \frac{\psi - \mu^2\chi}{\sqrt{2}(1-\mu^2)}, X_{22} = \frac{\phi - \mu^2\xi}{1-\mu^2}. \quad (14)$$

$$Y_{11} = \sigma, Y_{12} = \sqrt{2}\theta, Y_{21} = \frac{\varepsilon - \mu^2\sigma}{\sqrt{2}(1-\mu^2)}, Y_{22} = \frac{\eta - \mu^2\theta}{1-\mu^2}. \quad (15)$$

2.2. Accuracy verification of the problem solution. Total quantum yield of radiation

In the studies of *Ivchenko et.al.* (1980, 1981) and *Sobirov* and *Yuldashev* (1984), the law of conservation of the total radiation flux, incident and diffusely reflected from a semi-infinite medium, was used to verify the accuracy of analytical and numerical calculations.

If a monochromatic, plane-parallel radiation flux πF falls on the surface of the medium (at the boundary $\tau = 0$), then after multiple scattering, part of the radiation is diffusely reflected from the plane $\tau = 0$, and part of the flux diffusely exits the medium through the plane $\tau = 1$. The total fluxes of diffusely reflected and transmitted radiation from the medium (per unit surface area) are determined by the formulas:

$$\pi\Phi^{ref} = \int_0^1 \mu d\mu \int_0^{2\pi} d\varphi I^{ref}(\tau = 0, \mu, \varphi),$$

$$\pi\Phi^{trans} = \int_0^1 \mu d\mu \int_0^{2\pi} d\varphi I^{trans}(\tau = \tau_1, -\mu, \varphi), \quad (16)$$

where $I^{(ref)}(\tau = 0, \mu, \varphi)$ and $I^{(trans)}(\tau = \tau_1, -\mu, \varphi)$ are the intensities of diffusely reflected and transmitted radiation at the boundary of the medium, determined by Eq.(10).

Solving the radiative transfer equation (Eq.(1)) allows determining only the diffusely scattered part of the incident flux in the medium that has undergone single or multiple scattering. However, part of the incident flux passes through the medium without scattering, which is not considered in Eq.(1). The unscattered part of the primary radiation, without changing the direction of incidence, is attenuated by $\exp(-\tau_1/\mu_0)\pi F$ and exits the medium (*Chandrasekhar*, 1960). We define the ratios of these three fluxes to the incident flux and sum them:

$$\eta^{ref} = \frac{\Phi^{\mathrm{ref}}}{\mu_0 F(+0,\mu_0,\varphi_0)}, \eta^{trans} = \frac{\Phi^{\mathrm{trans}}}{\mu_0 F(+0,\mu_0,\varphi_0)}. \quad (17)$$

$$\eta^{total} = \eta^{ref} + \eta^{trans} + \exp\left(-\frac{\tau_1}{\mu_0}\right). \quad (18)$$

This formula defines the distribution of the primary flux for diffusely reflected, diffusely transmitted, and unscattered fluxes. In analogy to $\widetilde{\omega}_0$, which represents the quantum yield from single scattering, the quantity η_{total}, is called the total quantum yield of radiation in (*Ivchenko et.al.,* 1980). Below, we will adhere to this definition for η.

In the case of a conservative medium ($\widetilde{\omega}_0 = 1$), the total flux is conserved, so in Eq.(18) the condition $\eta_{\mathrm{total}} = 1$ must be satisfied. This condition holds regardless of the optical thickness of the medium, the angle of incidence of the incident flux, and serves as a criterion for assessing the accuracy of analytical and numerical calculations. On the other hand, the relationship described in Eq.(18) allows establishing the law of redistribution of the outgoing secondary flux from the medium depending on the optical thickness of the medium (from the wavelength of the incident radiation).

Table 1 presents the results of numerical calculation of the total quantum yield at various values of the illumination angle of atmospheric layers with natural, unpolarized solar radiation.

According to the data in *Table 1*, one can assess what proportion of the incident radiation is scattered, and what part is diffusely reflected back or passes through the medium. For example, at normal incidence, on average about 10% of the rays from the green part of the spectrum ($\tau_1 = 0.1,\ \lambda = 0.546\ \mu\mathrm{m}$) are scattered, and 90% pass through the medium without scattering. For violet rays ($\tau_1 = 0.5, \lambda = 0.37\ \mu\mathrm{m}$), the proportion of scattered rays increases to approximately 40%.

Table 1. Results of calculating the total quantum yield of diffusely reflected, transmitted, and unscattered radiation at various illumination angles and optical thicknesses, $\tilde{\omega}_0 = 1$

μ_0	η_{ref}	η_{trans}	$\eta_{ref} + \eta_{trans}$	$\exp(-\tau_1/\mu_0)$	η_{total}
		$\tau_1 = 0.001,\ \lambda = 1.670\ \mu m$			
0	0.50295806	0.4913439	0.99430193	0	0.9943019
0.2	0.01235285	0.0132404	0.02559321	0.9950124	1.0206056
0.4	0.00622429	0.0065941	0.01281842	0.9975031	1.0103215
0.6	0.00416402	0.0043620	0.00852599	0.9983347	1.0068607
0.8	0.00313426	0.0032165	0.00635071	0.9987507	1.0051014
1	0.00267292	0.0019598	0.00463271	0.9990005	1.0036332
		$\tau_1 = 0.01,\ \lambda = 0.920\ \mu m$			
0	0.508344001	0.4859448	0.99428885	0	0.99428885
0.2	0.024403672	0.0261452	0.05054884	0.9512294	1.00177826
0.4	0.012372619	0.0131070	0.02547959	0.9753099	1.00078950
0.6	0.008294686	0.0086864	0.01698112	0.9834715	1.00045258
0.8	0.006250375	0.0064061	0.01265651	0.9875778	1.00023431
1	0.005342862	0.0039199	0.00926272	0.9900498	0.99931256
		$\tau_1 = 0.1,\ \lambda = 0.546\ \mu m$			
0	0.57015844	0.4240466	0.9942055	0	0.9942050
0.2	0.19901661	0.2075493	0.4065658	0.6065306	1.0130965
0.4	0.11129502	0.1174036	0.2286986	0.7788007	1.0074994
0.6	0.07712613	0.0812964	0.1584225	0.8464817	1.0049043
0.8	0.05902330	0.0620124	0.1210357	0.8824969	1.0035326
1	0.04915566	0.0376694	0.0868205	0.9048374	0.9916625
		$\tau_1 = 0.5,\ \lambda = 0.371\ \mu m$			
0	0.68443190	0.2992614	0.98369334	0	0.98369333
0.2	0.51703888	0.4047164	0.92175532	0.0820858	1.00384031
0.4	0.37843796	0.3487235	0.72716148	0.2865048	1.01366627
0.6	0.29298172	0.2868027	0.57978439	0.4345982	1.01438266
0.8	0.23799182	0.2419630	0.47995479	0.5352614	1.01521622
1	0.20055734	0.1893865	0.38994375	0.6065306	0.99647436
		$\tau_1 = 1,\ \lambda = 0.312\ \mu m$			
0	0.73773050	0.2118047	0.94953523	0	0.9495352
0.2	0.62204550	0.3232367	0.94528369	0.0067380	0.9520216
0.4	0.51901118	0.3683299	0.88734110	0.0820850	0.9694261
0.6	0.43571001	0.3592421	0.79495200	0.1888756	0.9838277
0.8	0.37285681	0.3364988	0.70935550	0.2865048	0.9958604
1	0.32561385	0.2874323	0.61304610	0.3678794	1.0098093
		$\tau_1 \to \infty$			
0	0.992526938	0	0.992526938	0	0.992526938
0.2	0.999637976	0	0.999637976	0	0.999637976
0.4	0.999804808	0	0.999804808	0	0.999804808
0.6	0.999927438	0	0.999927438	0	0.999927438
0.8	1.000042373	0	1.000042373	0	1.000042373
1	1.000146482	0	1.000146482	0	1.000146482

From the table, it can be seen that in the long-wavelength part of the spectrum, regardless of the angle of incidence, the proportions of diffusely reflected and transmitted radiation in the total quantum yield are almost identical. In the short-wavelength part of the spectrum, diffusely reflected radiation predominates. This is explained by the fact that with increasing optical thickness of the medium, the flux of transmitted diffuse and unscattered radiation decreases.

For comparison, similar calculations were performed using the tabulated values of the $\psi, \varphi, \chi, \xi, \varepsilon, \eta, \sigma, \theta$ functions from the work of *Chandrasekhar* and *Elbert* (1954). The results of the calculations showed that when the medium is illuminated normally and near this point ($\mu_0 \to 1$), at all values of optical thickness, the value of the total quantum yield exceeds the expected value, reaching up to 9% in certain points (*Table 2.*). However, in our calculations, deviations are observed in the region $\mu_0 \to 1$, which are lower than expected and amount to up to 5%. The probable cause of the disappearance of part of the short-wavelength radiation is the insufficiently accurate accounting for the number of scatterings and the diffuse radiation exiting the medium at $\mu_0 \to 1$, in the iteration method. In the geometry of medium illumination when $\mu_0 \to 1$, short-wavelength radiation travels a long optical path in the medium and undergoes multiple scatterings. It is likely that in the iterative method of solving equations, part of the radiation is not taken into account, which may explain the observed deviation. In the case of a semi-infinite medium ($\tau_1 \to \infty$), the results of our calculations and those using Chandrasekhar's functions coincide, and the law of conservation of total flux is satisfied with high accuracy.

Table 2. Calculation results based on the values of the $\psi, \varphi, \chi, \xi, \varepsilon, \eta, \sigma, \theta$ functions in Chandrasekhar and Elbert (1954)

μ_0	η_{ref}	η_{trans}	$\eta_{ref} + \eta_{trans}$	$\exp(-\tau_1/\mu_0)$	η_{total}
			$\tau_1 = 0.2$		
0	0.61821120	0.3819794	1.00019055	0	1.00019055
0.20	0.32777708	0.3249194	0.65269643	0.3678794	1.02057587
0.44	0.18579127	0.1871951	0.37298640	0.6347364	1.00772282
0.68	0.12879399	0.1377657	0.26655965	0.7451888	1.01174847
0.92	0.09839073	0.1893681	0.28775880	0.8046151	1.09237385
1	0.09119335	0.1623395	0.25353290	0.8187308	1.07226365
			$\tau_1 = 1$		
0	0.765023981	0.2329303	0.99795427	0	0.9979543
0.20	0.648421603	0.3520141	1.00043574	0.0067379	1.0071737
0.44	0.524457435	0.3993407	0.92379817	0.1030308	1.0268290
0.68	0.427572533	0.3808561	0.80837256	0.2297903	1.0381628
0.92	0.357323733	0.4007442	0.75806795	0.3372413	1.0953093
1	0.338355703	0.3627337	0.70108936	0.3678794	1.0689688

According to the data in *Table 1*, it can be concluded that if calculations are carried out using Chandrasekhar's method, some difficulties can be expected in the calculations for $\mu_0 \to 1$, across the entire optical spectrum. Apparently, for this reason, Coulson's monograph does not consider the case, where the angle of incidence of the solar rays is normal to the surface of the medium and for values of angles close to the normal. When performing calculations using our method,

such discrepancies are observed only in the short-wavelength region of the spectrum at $\mu_0 \to 0$.

Coulson's monograph mentions that in the ultraviolet wavelength region, some difficulties are observed in the calculations. He attributes these difficulties to the data in Elterman's table.

The results in *Table 1* allow us to evaluate the proportion of incident radiation that is scattered, diffusely reflected back, or transmitted through the medium. For example, at normal incidence, approximately 10% of the rays from the green part of the spectrum ($\tau_1 = 0.1, \lambda = 0.546$ μm) are scattered, and 90% pass through the medium without scattering. For violet rays ($\tau_1 = 0.5, \lambda = 0.371\ \mu m$), the proportion of scattered rays increases to approximately 40%.

It can be seen from the table that in the long-wavelength part of the spectrum, regardless of the angle of incidence, the proportions of diffusely reflected and transmitted radiation in the total quantum yield are almost identical. In the short-wavelength part of the spectrum, diffusely reflected radiation predominates. This is because, with increasing optical thickness of the medium, the flux of transmitted diffuse and unscattered radiation decreases.

3. Calculation of the angular characteristics of the secondary radiation intensity considering various orders of scattering

The incident unpolarized radiation has the following Stokes parameters:

$$F_l = F_r = (1/2)F, F_U = F_V = 0, \tag{19}$$

and the degree of linear polarization of diffusely reflected and transmitted radiation is determined by the formula:

$$P_{lin} = (I_l - I_r)/(I_l + I_r). \tag{20}$$

Figs. 1 – 4 show the results of calculations of the angular characteristics of the degree of linear polarization of diffusely reflected and transmitted radiation from the medium. The incident, reflected, and transmitted radiation lie in the same meridional plane, in the plane of the solar vertical.

Fig. 1 shows the results of the calculation of the angular distribution of the degree of polarization of transmitted radiation for various illumination angles. For comparison, calculations were made using Coulson's parameters (see Figure 4.6 in *Coulson* (1988)) at an optical thickness of $\tau_1 = 0.15$ ($\lambda = 0.495$ μm).

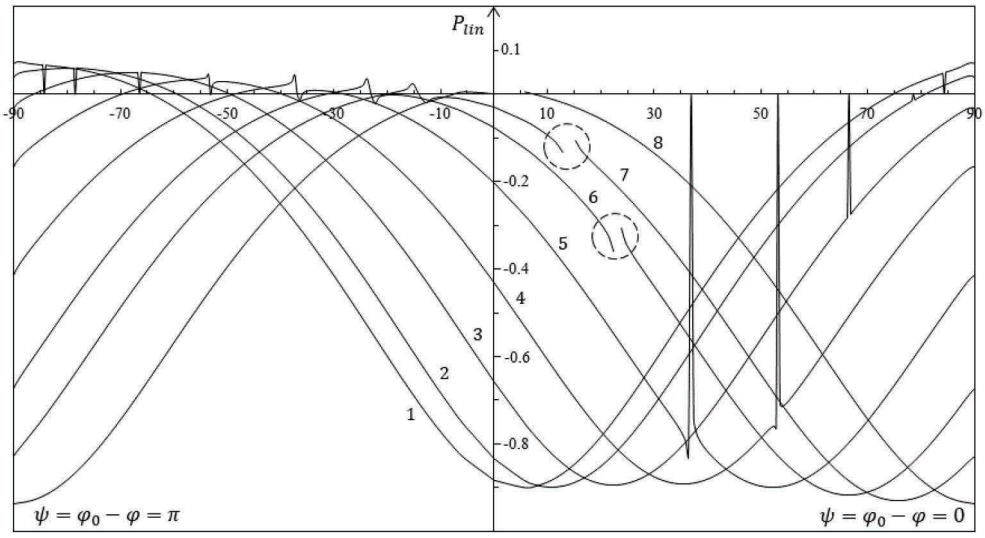

Fig. 1. Angular distribution of the degree of polarization of diffusely transmitted radiation at various illumination angles. Curves 1–8 are calculated for medium illumination angles μ_0= 0.1, 0.2, 0.4, 0.6, 0.8, 0.92, 0.97, respectively, at τ_1 = 0.15 (λ = 0.495 μm), $\tilde{\omega}_0 = 1$. The calculations are based on the Coulson's parameter values (Figure 4.6 in *Coulson* (1988)).

It can be observed that all angular distributions of the degree of polarization, calculated at different illumination angles, coincide with Coulson's results with high accuracy. However, in our calculations, when the polar illumination angle is equal to the observation angle ($\tilde{\mu} = \mu = \mu_0$), an anomaly is observed in the value of the degree of polarization. Near this point, the degree of polarization changes abruptly. For a clearer representation of this phenomenon, in curves 6 and 7, the regions around the point $\tilde{\mu}$, where the degree of polarization behaves anomalously, are highlighted separately.

With a change in the angle of illumination, the width of the anomalous region changes: it decreases when $\mu_0 \to 0$ and increases when $\mu_0 \to 1$.

For comparison, in *Fig. 2*, the results of similar calculations of the angular distribution of the degree of polarization are presented for an optical thickness of $\tau_1 = 1$ ($\lambda = 0.312$ μm). From the figure, it is evident that with an increase in optical thickness, the angular width of the anomalous region expands, and the jump in the degree of polarization value around the point $\tilde{\mu} = \mu = \mu_0$ increases.

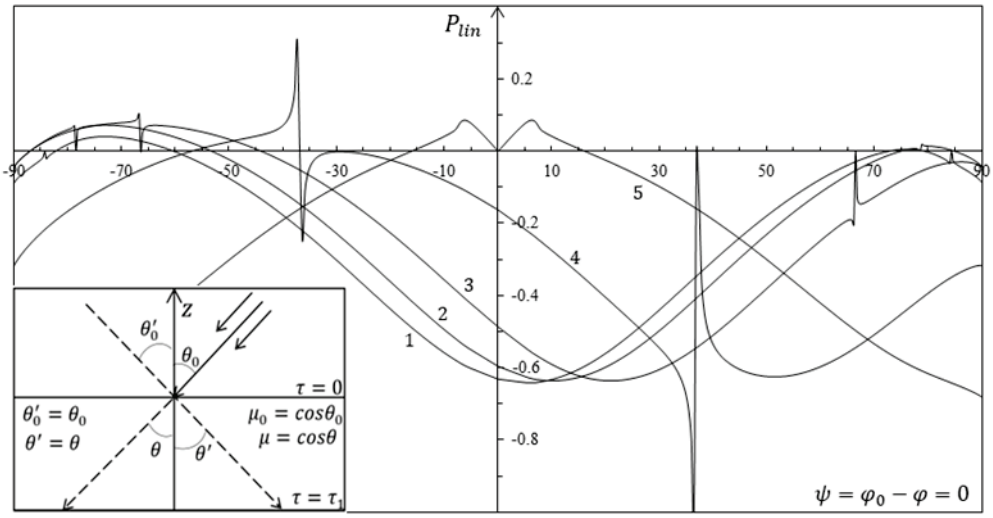

Fig. 2. Angular distribution of the degree of polarization of diffusely transmitted radiation at various illumination angles. Curves 1–5 are calculated for medium illumination angles μ_0= 0.1, 0.2, 0.4, 0.8, 1, respectively, at τ_1 = 1 (λ = 0.312 μm), $\tilde{\omega}_0 = 1$.

For the parameters $\tau = 1$ and $\mu_0 \approx 0.8$, the angular width of the anomalous region in the half-plane $\psi = \pi$ is $\Delta\tilde{\theta} \approx 4°$, and in the half-plane $\psi = 0$, $\Delta\tilde{\theta} \approx 6°$. In the case of $\tau = 0.15$ and $\mu_0 \approx 0.8$, the angular widths are $\Delta\tilde{\theta} \approx 1°$ and $\Delta\tilde{\theta} \approx 3°$, respectively. The angular width of the anomalous region in the solar plane is larger than in the anti-solar half-plane.

In the geometry of normal illumination and observation ($\mu = \mu_0 = 1$), the degree of polarization is zero. The jump in the degree of polarization takes on a symmetrical form. With a deviation of the observation angle from the normal, at $\mu < 1$, the degree of polarization first assumes a positive value, then it transitions to the negative region through neutral points.

The anomaly in the degree of polarization is observed for all values of optical thickness, as well as in the case of a non-conservative medium ($\tilde{\omega}_0 < 1$). With a decrease in the albedo value, the anomalous polarization diminishes.

It should be noted that the aforementioned feature is observed for all azimuthal angles of the hemisphere around the lower boundary of the atmosphere at $\tilde{\mu} = \mu = \mu_0$.

The presence of a singularity in the solutions of the transfer equation for transmitted radiation at $\tilde{\mu} = \mu = \mu_0$ is known (*Natraj et.al.,* 2009; *Kattawar et al.,* 1976), but in these works, the jump in the degree of polarization around this point is not discussed. Apparently, this feature was not established. If the indicated jump in the degree of polarization is indeed observed, then during observations through a polarimeter along the solar vertical, it is possible to detect a difference in the degree of polarization of solar radiation at symmetric points near the sun. This

feature was observed during double Mandelstam-Brillouin scattering of exciton polaritons in crystals with cubic symmetry (*Ivchenko* and *Sobirov,* 1985).

In the angular distribution of the degree of polarization along the plane of the solar vertical, at certain points, the degree of polarization changes sign, with the degree of polarization equaling zero at these points. These neutral points (Brewster, Babinet, and Arago) serve as indicators of the atmospheric state. Besides these points, the presence of a fourth point, near the Arago point, was also proposed. The presence of double Arago points was theoretically first shown in the work of *Dave* and *Furukawa* (1966) when studying the scattering of ultraviolet rays in the atmosphere. However, these calculations were performed outside the framework of the $X(\mu), Y(\mu)$–function theory. This point was discovered in observations only recently, in 2002, and the topic of neutral points constantly remains in the focus of specialists (*Horvath et al.,* 2002; *Horvath et al.,* 2011).

Unlike the Brewster and Babinet points, the observation of double Arago points requires higher orders of scattering. For this reason, these points are observed only in the short-wave part of the optical spectrum. Our calculation results show that the presence of double Arago points can be demonstrated within the framework of the $X(\mu), Y(\mu)$ – function theory in the range of illumination angle values $0 < \mu_0 \leq 0.2$ and optical thickness $0.85 < \tau_1 < 1.15$. *Fig. 3* shows the formation of double Arago points in the angular distribution of the degree of polarization of transmitted radiation, depending on the number of scatterings. It should be noted that Coulson's works discuss only one Arago point.

Fig. 4 presents the results of calculations of diffusely reflected solar radiation from atmospheric layers for the parameter values used in *Fig. 1*. For all values of illumination and observation angles, as well as optical thicknesses, in the angular polarization characteristics of diffusely reflected radiation, a jump in the degree of polarization is not observed, with only one Arago point being present.

In conclusion, it should be noted that the developed method for calculating the $X(\mu), Y(\mu)$ – functions significantly simplifies the calculation of the intensity and degree of polarization of diffusely reflected and transmitted solar radiation from atmospheric layers for all points of the hemisphere adjacent to the lower and upper surfaces of the atmosphere.

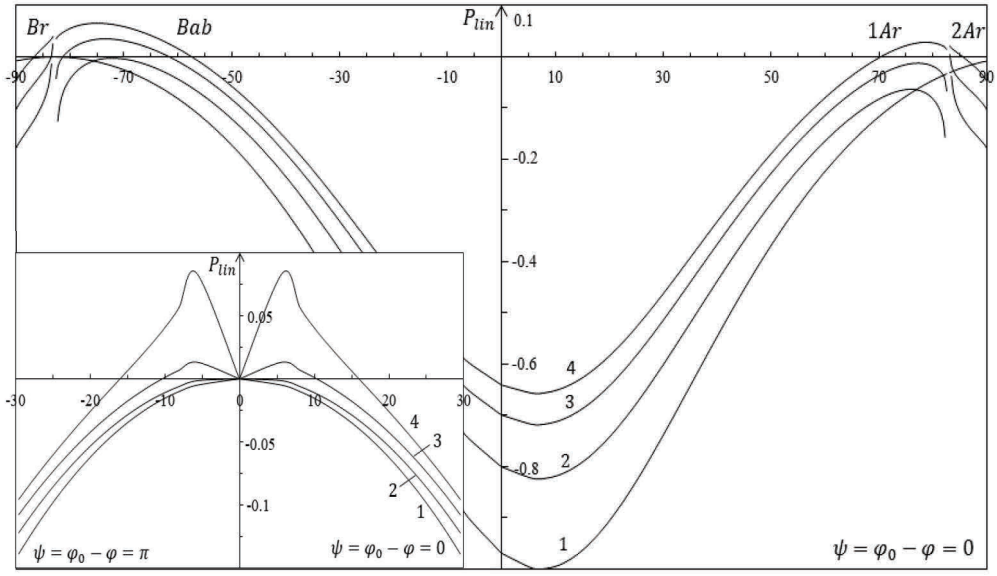

Fig. 3. Formation of double Arago points depending on the number of scatterings. Curves 1–4 correspond to the number of iterations n = 1, 2, 3, 4 (scattering order ν = 1, 3, 7, 15,respectively) for $\tau_1 = 0.9$ and $\mu_0 = 0.125$. The inset shows the formation of the region with positive polarization depending on the multiplicity of scattering for $\tau_1 = 1$ and $\mu_0 = 1$ (curve 5 in *Fig. 2*).

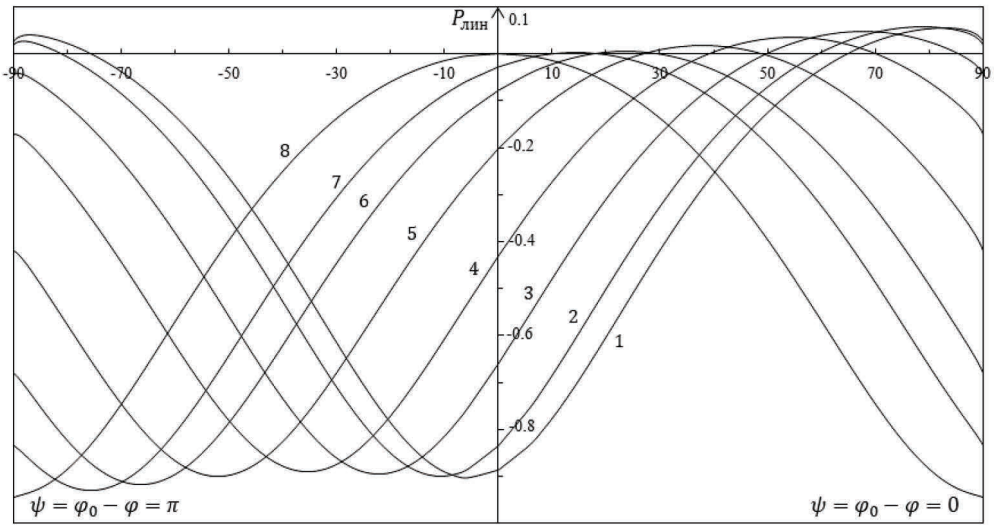

Fig. 4. Angular distribution of the degree of polarization of diffusely reflected radiation at different illumination angles. Curves 1–8 are calculated for the parameter values indicated in *Fig. 1*.

4. Conclusions

1. The solutions of the radiative transfer equation for polarized radiation in a medium with finite optical thickness, obtained using the factorization method, have been analyzed. Based on the obtained equations, the angular distribution of the degree of polarization of diffusely reflected and transmitted radiation from layers of the atmosphere of natural, unpolarized solar radiation along the solar vertical was investigated.

2. It has been shown that in the case of forward scattering of incident radiation, a feature is observed in the angular distribution of the degree of polarization of diffusely transmitted radiation. At μ=μ_0, the degree of polarization of the transmitted radiation changes abruptly within a narrow angular width of observations.

3. The positions of neutral points in the angular characteristics of secondary radiation have been studied. It has been shown that in certain regions of illumination angle and optical thickness values in the angular distribution of the degree of polarization of diffusely transmitted radiation, it is possible to simultaneously observe two Arago points.

4. The results of numerical calculations show that the iteration method is an effective method for determining the numerical values of the *X(μ), Y(μ)* functions obtained by the factorization method. The calculation method is very simple and does not require a long time for computer computations.

ORCID:
Jurabek Y. Rozikov, https://orcid.org/0000-0003-3820-2962
Makhmud M. Sobirov, https://orcid.org/0000-0002-6447-0728
Valijon U. Ruziboyev, https://orcid.org/0000-0002-6199-1165

References

Chandrasekhar, S., 1960: Radiative transfer. Dover Publications Inc, New York

Natraj, V., Li, *K.F.,* and *Yung*, *Y.L.,* 2009: Rayleigh scattering in planetary atmospheres: Corrected tables through accurate computation of *X* and *Y* functions. *The Astrophysical Jornal*, 691:1909-1920. https://doi.org/10.1088/0004-637X/691/2/1909

Natraj, V. and *Hovenier, J.W.*, 2012: Polarized light reflected and transmitted by thick Rayleigh scattering atmospheres. *The Astrophysical Journal*, 748:28 (16pp). https://doi.org/10.1088/0004-637X/748/1/28

Chandrasekar, S. and *Elbert, D.D.,* 1954: The illumination polarization of the sunlit sky on Rayleigh scattering. *Transactions of the American Philosophical Society, New Series 44*(6) 643-728.

Coulson, K.L., 1988: Polarization and intensity of light in the atmosphere. A. Deepak Publishing, Hampton, VA.

Coulson, K.L., Dave, J.V., and *Sekera, Z.*, 1960: Tables Related to Radiation Emerging from a Planetary Atmosphere with Rayleigh Scattering. Univ. California Press, Berkeley, CA

Yan, L., Yang, B., Zhang, F., Xiang, Y., and *Chen, W*., 2020: Polarization Remote Sensing Physics. Peking University Press. Springer. https://doi.org/10.1007/978-981-15-2886-6

Yan, L., Wu, T., and *Wang, X*., 2019: Polarization Remore Sesing for Land Observation. In Understanding of Atmospheric Systems with Efficient Numerical Methods for Observation and Prediction. IntechOpen. https://doi.org/10.5772/intechopen.79937

Mishchenko, M.I., 1987: Electromagnetic Scattering in Random Dispersive Media: Fundamental Theory and Applications (PhD thesis). National Academy of Sciences of Ukraine (published 2012). (in Russian)

Mishchenko, M.I., Travis, L.D., and *Lacis, A.A.,* 2006: Multiple scattering of light by particles: Radiativ transfer and coherent backscattering. Cambrige University Press

Sobirov, M.M. and Rozikov, J.Y., 2020: Nekotoriye voprosi teorii perenosa polyarizovannogo izlucheniya v izotropnoy srede s konechnoy opticheskoy tolshinoy. *Nauchno - texnicheskiy jurnal, Ferganskiy PI 24* (4), 15-24. (in Russian)

Lenoble, J., 1970: Importance de la polarization dans le rayonnement diffuse par une atmosphere planetair. *Journal of Quantativ Spektroskopy and Radiativ Transfer 10*, 533–551. (in French)

Ivchenko, Y.L., Pikus, G.Y., and *Yuldashev, N.X.,* 1980: Perenos polyarizovannogo izlucheniya v kristallax v eksitonnoy oblasti spektra. Vliyaniye pereizlucheniya. *Jurnal eksperimentalnoy i teoreticheskoy fiziki 79*, 1573-1590. (in Russian)

Ivchenko, Y.L., Pikus, G.Y., and *Yuldashev, N.X.,* 1981: Perenos polyarizovannogo izlucheniya v kristallax v eksitonnoy oblasti spektra. Poyaritonniye effekti. *Jurnal eksperimentalnoy i teoreticheskoy fiziki 80*, 1228-1246. (in Russian)

Sobirov, M.M. and *Yuldashev, N.X.,* 1984: Teoriya perenosa polyarizovannogo izlucheniya v kubicheskix kristallax v prodolnom magnitnom pole v oblasti eksitonnogo rezonansa. *Jurnal eksperimentalnoy i teoreticheskoy fiziki 87*, 677-690. (in Russian)

Pikus, G.Y., Sobirov, M.M., and *Yuldashev, N.X.*, 1985: Kinetika polyarizovannogo izlucheniya pri rezonansnom impulsnom vozbujdenii eksitonov v kristallax. *Jurnal eksperimentalnoy i teoreticheskoy fiziki 97*, 635-641.

Elterman, L., 1968: UV, visibe, and IR attenuation for altitudes to 50 km. *AFCRL-68-0153, Env. Res. Pap. No. 285.* U.S. Air Force.

Sobirov, M.M., Rozikov, J.Y., and *Ruziboyev, V.U.,* 2021: Polyarizatsionniye xarakteristiki diffuzno otrajennogo i propushyennogo izlucheniya v srede s konechnoy opticheskoy tolshinoy. Uzbekskiy fizicheskiy jurnal 23(2) 11-20. https://doi.org/10.35134/jitekin.v11i1.26

Sobirov, M. M., Rozikov, J. Y., Yusupova, D. A., and *Ruziboyev, V. U.*, 2023: Calculation of spectral and angular distribution of diffusely reflected, diffusely transmitted, and unscattered fluxes of solar radiation in atmospheric layers. *Applied Solar Energy 59(5)*, 761–769. https://doi.org/10.3103/S0003701X23601187

Sobirov M. M., Rozikov J. Y., Ruziboyeva, V. U., and *Kamolova, M.M.,* 2024: Calculation of the Spectral and Angular Distribution of Diffusely Reflected and Transmitted Solar Radiation Fluxes from Atmospheric Layers. Problems in the Textile and Light Industry in the Context of Integration of Science and Industry and Ways to Solve Them AIP Conf. Proc. 3045, pp.020008-1–020008-5. https://doi.org/10.1063/5.0197368

Kattawar, G.W., Plass, G.N., and *Hitzfelder, S.J.,*1976: Multiple scattered radiation emerging from Rayiegih and continental haze layers. Radiance, polarization, and neutral points. *Applied Optics 15(3),* 632-647. https://doi.org/10.1364/AO.15.000632

Ivchenko, Y.L. and *Sobirov, M.M.,* 1985: Osobennost v spektre dvuxfononnogo Mandelshtamm - Brillyuenovskogo rasseyaniya nazad. *Fizika tvyordogo tela 27*, 1096-1104. (in Russian)

Dave, J.V. and *Furukawa, P. M.,* 1966: Intensity and polarization of the radiation emerging from an optically thick atmosphere. *Journal of the Optical Society of America 56*, 394-400. https://doi.org/10.1364/JOSA.56.000394

Horvath, G., Bernath, B., Suhai, B., Barta, A., and *Wehner, R*., 2002: First observation of the fourth neutral polarization point in the atmosphere. *Journal of the Optical Society of America 19(10)*, 2085–2099. https://doi.org/10.1364/JOSAA.19.002085

Horvath, G., Bernath, B., Suhai, B., Barta, A., and *Wehner, R*., 2011: Neutral points in an atmosphere–ocean system. 2: Downwelling light field. *Applied Optics 50(3),* 335–346. https://doi.org/10.1364/AO.50.000335